

Runaway Electron Beam Formation in Coaxial Gas-Filled Diode¹

V.V. Ryzhov, K.P. Artemov, S.Ya. Belomyttsev, A.A. Grishkov,
I.Yu. Turchanovskii, and V.A. Shklyaev

*Institute of High Current Electronics SB RAS, 2/3, Akademichesky ave., Tomsk, 634055, Russia
Phone: 8(3822) 49-14-71, Fax: 8(3822) 49-24-10, E-mail: ryzhov@to.hcei.tsc.ru*

Abstract – The formation of the runaway electron beam in the coaxial gas-filled diodes was studied by computer simulation with PIC codes KARAT and OOPIC Pro. The runaway electron current dependence of pressure for the different diode schemes was obtained. It has been shown that the runaway electron is generated mostly in cathode region. The emission process affect to the current and duration of the runaway electron pulse was studied.

1. Introduction

Recently, the formation of a subnanosecond fast electron beam in a high-pressure gas has again attracted the attention of researchers [1–8]. It is shown experimentally [1] that in a gas-filled diode at atmospheric pressure with a highly nonuniform field at the cathode, a beam of runaway electrons of width no greater than 50 ps is formed in the near-cathode region on application of a subnanosecond voltage pulse. There are two main models explaining the mechanism for the formation of a runaway electron beam at the cathode or in the near-cathode region. The first model [2] assumes that the main process responsible for the electron beam formation under these conditions is field emission from microedges of the cathode. According to the model, the beam is formed at the time interval between the instant the voltage pulse is applied and the onset of explosive electron emission from the cathode, with the beam width limited to ~ 10 ps by the field-to-explosive emission transition time. The second model [3], which is based on numerical simulation of the processes occurring near the cathode, gives the same explanation of the electron beam formation under these conditions. However, calculations suggest that the beam consists mainly of electrons resulting from gas ionization near the cathode, the width of the runaway electron beam is 10–20 ps and is limited due to shielding of the nonuniform external electric field near the cathode by the gas-discharge plasma.

At the same time, with the assumption of limitless cathodes emissivity, one should expect changes in the conditions of beam formation and in the current of fast electrons, as well as another causes for limited beam width. The mechanism for the formation of a fast electron beam in a gas-filled diode was studied using the electromagnetic PIC code OOPIC Pro [9].

2. Diode geometry

Schematic of the computational domain is shown in Fig. 1. The system comprises a cylindrical cathode with an outer diameter of 10 mm, and a length of the cylindrical section of 70 mm. The cathode is inside an anode chamber of inner radius 60 mm. The gap between the cathode edge and the anode wall is 20 mm. A voltage pulse of amplitude 150 kV, rise time 300 ps, and duration 3 ns is applied to the diode. Calculations were performed for both vacuum and gas-filled systems. The working gas was helium. In the calculation, the gas pressure was varied from vacuum to 800 torr. The objective of the work was to simulate the formation of a fast electron beam in a gas-filled diode for limitless cathode emissivity.

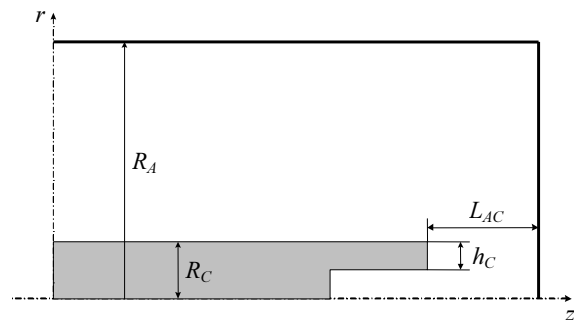


Fig. 1. Schematic of the computational domain: anode tube radius $R_A = 60$ mm, cathode radius $R_C = 10$ mm, cathode thickness $h_C = 5$ mm, cathode edge – anode separation $L_{AC} = 20$ mm, voltage at the entry of the computational domain 150 kV, voltage pulse rise time 300 ps, voltage pulsewidth 3 ns

3. Results

In the program used, there was no possibility to simulate the passage of a fast electron beam through a foil, and therefore we employ a boundary condition allowing separation of the electron current into the current of electrons with an energy at the anode greater than 50 keV and the current of slow plasma electrons. This boundary condition was used for comparing the simulation results with available experimental data in which the anode was a foil absorbing low-energy electrons [1, 4–6].

¹ The work was supported by the Russian Foundation for Basic Research (Grant No. 06-08-00637-a).

3.1. Dynamics of the beam and plasma formation

Figure 2 shows phase portraits of electrons at different points in time. The ordinate is the particle momentum ($P = \gamma v$, where γ is the relativistic factor of a particle, v is the particle velocity) and the abscissa is a coordinate along the z axis. It is seen from the phase portraits that under these conditions, first fast electrons reach the anode at the time interval between 500 and 600 ps. At the point in time 800 ps, the plasma of average electron energy less than 10 eV fills the gap.

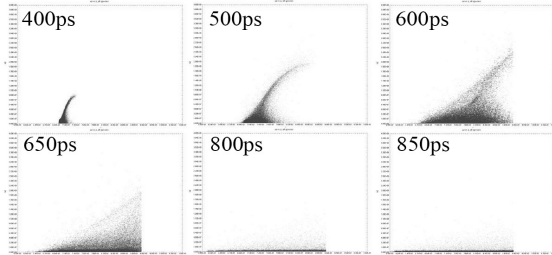


Fig. 2. Phase portraits at different points in time: voltage at the entry of the computational domain 150 kV, voltage pulse rise time 300 ps, gas – helium, gas pressure 200 torr, voltage pulsewidth 3 ns

Figure 2 shows the plasma distributions (the distributions of the He ion density in the cathode-anode gap) at different points in time. The distributions are bounded from above by $5 \cdot 10^{19} \text{ m}^{-3}$.

Note that the generation of a fast electron beam in a gas-filled diode should be considered taking into account not only phase portraits at different points in time, but also plasma distributions corresponding to these points. Analysis of the distributions makes clear that fast electrons of energy close to the applied voltage move toward the region with no dense plasma.

It is seen from the phase portrait and plasma distribution at 600 ps that by this time first fast electrons reach the anode, the plasma density near the cathode is four orders of magnitude different from that near the anode. At the instant the electron beam current cuts off, the gap is almost entirely filled by a dense plasma of density $1 \cdot 10^{19} \text{ m}^{-3}$.

At $t \geq 800$ ps, the cathode-anode gap is filled by a dense plasma of density about $3^{-5} \cdot 10^{19} \text{ m}^{-3}$ (see Fig. 3) and the average electron energy in the plasma channel at this point in time is 5–8 eV. It also follows from Fig. 3 that at the instant the fast electrons arrive at the anode (500–600 ps), the dense plasma does not fill even a quarter of the cathode-anode gap. Thus, in the coaxial gas-filled diode, the mechanism of electron acceleration (named the “compressed capacitor mechanism”), where the dense plasma from the cathode forces the field toward the near-anode region in which conditions are established for the generation of a fast electron beam [5], is not realized. This is due to smearing of the dense plasma boundary in preliminary ionization of the gap by fast electrons. For this reason, no clearly defined boundary of the dense plasma was

found in the calculations. These results agree well with data of [1, 3, 4] in which the beam of fast electrons is shown to form near the cathode.

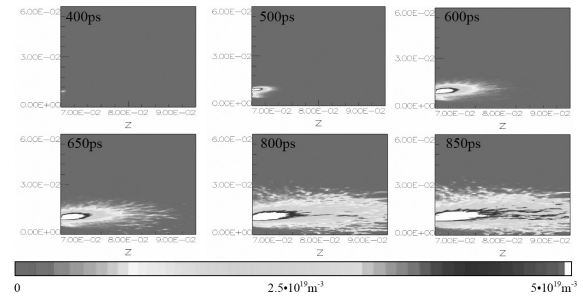


Fig. 3. Distribution of He ion density in the cathode-anode gap at different points in time: voltage at the entry of the computational domain 150 kV, voltage pulse rise time 300 ps, gas – helium, gas pressure 200 torr, voltage pulsewidth 3 ns

3.2. Energy and angular distributions of electrons

Figures 4 and 5 show integral energy distributions of fast electrons with an energy greater than 50 keV at the point in time 550 ps (first fast electrons have reached the anode) and at 700 ps (current is transferred not only by fast electrons, but by slow plasma electrons as well). Computer simulation shows that the spectrum consists of two regions, of which one is formed by fast electrons with the average energy approximating the applied voltage and the other by low-energy plasma electrons. Note that in the spectrum of fast electrons, electrons of energy greater pressure 200 torr, voltage pulsewidth 3 ns. than the applied voltage are found. However, they are few with respect to all fast electrons and their energy is greater than the applied voltage by a mere 10%, which fully fits the concept of the possibility to increase the energy of fast electrons [3].

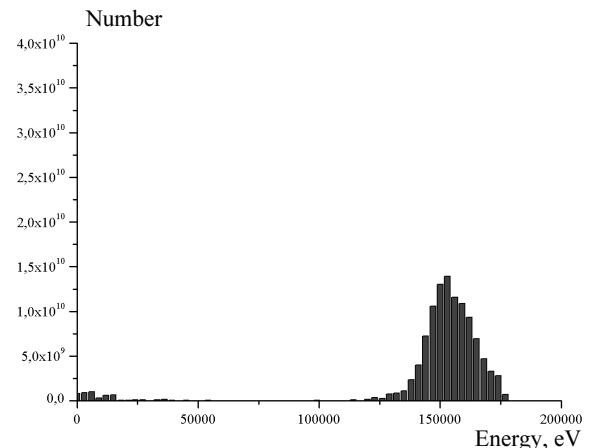


Fig. 4. Electron energy distribution at 550 ps: voltage at the entry of the computational domain 150 kV, voltage pulse rise time 300 ps, gas – helium, gas pressure 200 torr, voltage pulsewidth 3 ns

Figures 6 and 7 show integral angular distributions for vacuum and gas-filled diodes. It is seen from the distributions that in geometrical terms, the beam can-

not be considered unidirectional even in the vacuum diode.

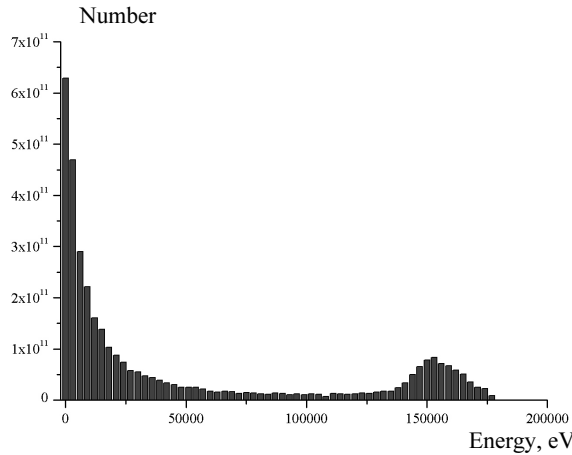


Fig. 5. Electron energy distribution at the anode at 700 ps: voltage at the entry of the computational domain 150 kV, voltage pulse rise time 300 ps, gas – helium, gas pressure 200 torr, voltage pulsewidth 3 ns

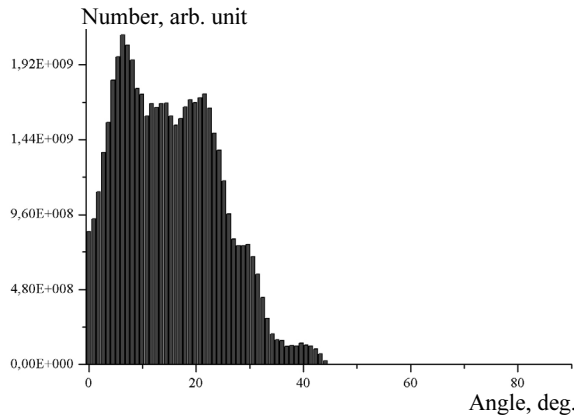


Fig. 6. Integral angular electron distribution at the anode in the vacuum diode: voltage at the entry of the computational domain 150 kV, voltage pulse rise time 300 ps, voltage pulsewidth 3 ns, calculation by the PIC code OOPIC Pro

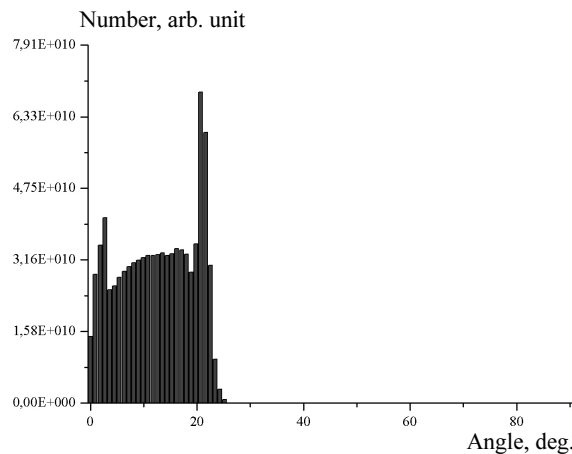


Fig. 7. Integral angular electron distribution at the anode at 550 ps: voltage at the entry of the computational domain 150 kV, voltage pulse rise time 300 ps, gas – helium, gas pressure 200 torr, voltage pulsewidth 3 ns, calculations by the PIC code OOPIC Pro

Computer simulations show that increasing the pressure further broadens the angular distribution spectrum. It should be noted that if we consider only fast electrons with energy corresponding to the maximum applied voltage, rather than all fast electrons, their angular distribution changes but lightly and the spectrum broadening with increasing the pressure is mainly due to electrons of energy only slightly higher than the threshold energy (50 keV).

3.3. Oscillograms of the current and voltage

Figure 8 shows oscillograms of the voltage at the entry of the computational domain and at the cathode. The time dependences of the current of fast electrons with an energy at the anode greater than 50 keV and of the total diode current are shown in Fig. 9. In all calculations, the voltage at the entry of the computational domain was constant. The diode impedance varied with pressure, thus changing the cathode voltage

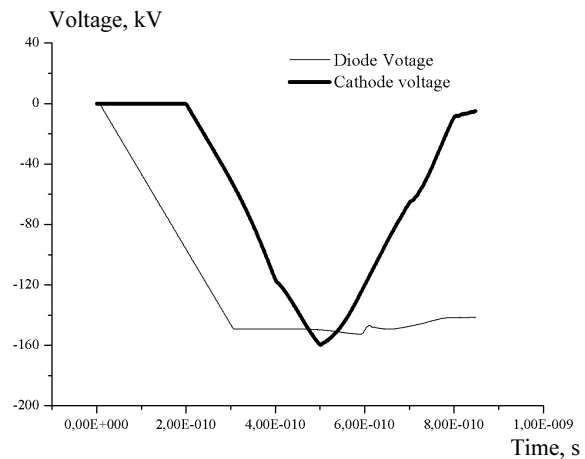


Fig. 8. Time dependence of the voltage at the entry of the computational domain and at the cathode: voltage at the entry of the computational domain 150 kV, voltage pulse rise time 300 ps, gas – helium, gas pressure 100 torr, voltage pulsewidth 3 ns

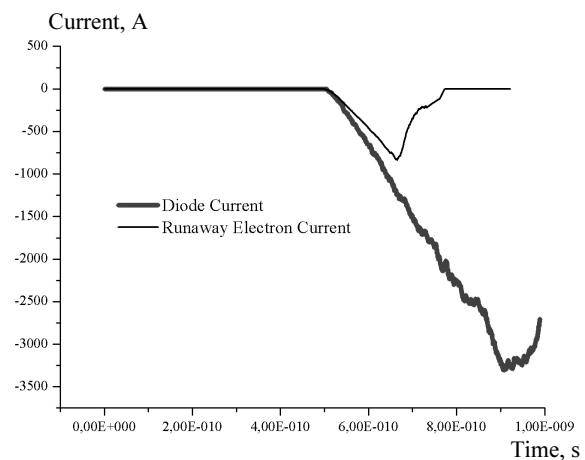


Fig. 9. Time dependence of the current of fast electrons with energy greater than 50 keV at the anode: voltage at the entry of the computational domain 150 kV, voltage pulse rise time 300 ps, voltage pulsewidth 3 ns

monitored using the corresponding diagnostic procedure. Note that the current of fast electrons was determined when the voltage dropped and this current corresponded to the arrival of first fast electrons, which are clearly seen on the phase portrait and particle distribution in the gap. The calculations show that the pulsewidth for fast electrons is about 200 ps. It is readily seen on the oscillogram of the current that at the initial point in time the total current is transferred only by fast electrons, and 150–200 ps later, mainly by slow plasma particles.

3.4. Pressure dependence of the beam current

Figure 10 shows the pressure dependence of the current of fast electrons with an energy at the anode greater than 50 keV for different gases.

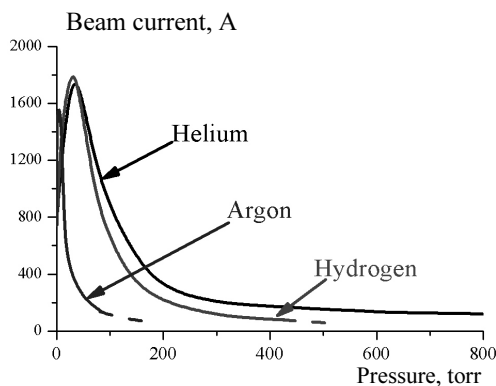


Fig. 10. Pressure dependence of the current of fast electrons with energy greater than 50 keV at the anode for different gases: voltage at the entry of the computational domain 150 kV, voltage pulse rise time 300 ps, voltage pulsewidth 3 ns

It is seen from the figure that the dependence is a characteristic curve with a maximum in the low-pressure range (tens of torr) and a plateau in the high-pressure range. As the gas pressure tends to zero, all three curves converge to a point corresponding to the current of the vacuum diode. The maximum on the curves results from gas amplification by ionization, namely from the increase in charge carriers at moderate pressures and relatively small retarding force. As the pressure builds up, the retarding force increases and the number of fast electrons decreases. The shape of the curve suggests that at high pressures (greater than 300 torr for helium), the current of fast electrons

depends weakly on pressure. As shown in [1, 3], the fact is that fast electrons under these conditions are formed mainly near the cathode and the number of runaway electrons remains near constant. The slope on the curve is explained as follows. As the gas pressure is increased, the retarding force increases and part of fast electrons loses their energy during the transport to the anode. The shape of the curve is circumstantial evidence that most of fast electrons fly out of the cathode or arise in the near-cathode region. The simulation results and instantaneous phase portraits confirm this conclusion.

4. Conclusion

Thus, in this work, we simulated the formation of fast electrons in a coaxial gas-filled diode for limitless cathode emissivity using the PIC code OOPIC Pro. It is shown that fast electrons are formed near the cathode, rather than near the anode, as the dense plasma approaches the anode. For the parameters under study, the mechanism of electron acceleration named the “compressed capacitor mechanism” is not realized in the coaxial gas-field diode. This is due to smearing of the dense plasma boundary in preliminary ionization of the gap by fast electrons.

References

- [1] G.A. Mesyats, V.G. Shpak, S.A. Shunailov, and M.I. Yalandin, *Pis'ma Zh. Tekh. Fiz.* **34**, 169 (2008).
- [2] G.A. Mesyats, *Pis'ma Zh. Eksp. Teor. Fiz.* **85**, 109 (2007).
- [3] S.Ya. Belomyttsev, I.V. Romanchenko, V.V. Ryzhov, and V.A. Shklyayev, *Pis'ma Zh. Tekh. Fiz.* **34**, 367 (2008).
- [4] G.A. Mesyats, S.D. Korovin, K.A. Sharypov et al., *Pis'ma Zh. Tekh. Fiz.* **32**, 18 (2006).
- [5] V.F. Tarasenko and S.I. Yakovlenko, *Usp. Fiz. Nauk* **47**, 887 (2004).
- [6] E.Kh. Baksht, V.F. Tarasenko, M.I. Lomaev, and D.V. Rybka, *Pis'ma Zh. Tekh. Fiz.* **33**, 373 (2007).
- [7] A.N. Tkachev, A.A. Fedenev, and S.I. Yakovlenko, *Tech. Phys.* **50**, 447 (2005).
- [8] L.P. Babich, *Usp. Fiz. Nauk* **175**/10, 1069 (2005).
- [9] J.P. Verboncoeur, A.B. Langdon, and N.T. Gladd, *Comp. Phys. Comm.* **87**, 199 (1995).